Journal of Bionic Engineering
https://doi.org/10.1007/s42235-023-00339-9

RESEARCH ARTICLE

An EMG-Based Biomimetic Variable Stiffness Modulation Strategy for Bilateral Motor Skills Relearning of Upper Limb Elbow Joint Rehabilitation

Ziyi Yang[1] · Shuxiang Guo[1,2] · Keisuke Suzuki[1] · Yi Liu[3] · Masahiko Kawanishi[4]

Received: 11 October 2022 / Revised: 25 December 2022 / Accepted: 4 January 2023

Abstract
Bilateral rehabilitation systems with bilateral or unilateral assistive robots have been developed for hemiplegia patients to recover their one-side paralysis. However, the compliant robotic assistance to promote bilateral inter-limb coordination remains a challenge that should be addressed. In this paper, a biomimetic variable stiffness modulation strategy for the Variable Stiffness Actuator (VSA) integrated robotic is proposed to improve bilateral limb coordination and promote bilateral motor skills relearning. An Electromyography (EMG)-driven synergy reference stiffness estimation model of the upper limb elbow joint is developed to reproduce the muscle synergy effect on the affected side limb by independent real-time stiffness control. Additionally, the bilateral impedance control is incorporated for realizing compliant patient–robot interaction. Preliminary experiments were carried out to evaluate the tracking performance and investigate the multiple task intensities' influence on bilateral motor skills relearning. Experimental results evidence the proposed method could enable bilateral motor task skills relearning with wide-range task intensities and further promote bilateral inter-limb coordination.

Keywords Biomimetic stiffness modulation · Compliant physical human–robot interaction (pHRI) · Electromyography (EMG) · Variable stiffness actuator (VSA) · Rehabilitation robotics · Synergy-based control · Skill relearning

1 Introduction

Bilateral rehabilitation has become a promising approach for the motor recovery of hemiplegia patients who have one side disability, as it can use the healthy side motions as reference guidance to improve the control ability of the affected side limb and further promote bilateral limb coordination [1–3]. With the rapid development and progression of artificial intelligence and big data processing and computation during the past decades, robotics-mediated bilateral rehabilitation systems [4], including end-effector type robots [5, 6], exoskeleton-type robots [7–9], and different driven-type robots [10], have been developed for providing repeatable, precisive, and high-efficient rehabilitation training [11]. Significantly, the bilateral rehabilitation robotic systems not only assist the affected side limb to complete the bilateral training task but also emphasize facilitating the natural inter-limb coordination between bilateral limbs that enable the hemiplegia to relearn the lost special bimanual motor skills [12, 13].

For this purpose, a common way to implement bilateral rehabilitation systems is to assist the bilateral limbs of hemiplegia patients to complete the synchronic and symmetric training task, including the axial symmetric force matching task or central symmetric trajectory tracking task [14]. In the force match task, the bilateral rehabilitation system should assist the output force coordination of bilateral limbs for completing the predefined bilateral training task [15]. Additionally, the bilateral rehabilitation robots are supposed

✉ Shuxiang Guo
guoshuxiang@hotmail.com

✉ Keisuke Suzuki
suzuki.keisuke@kagawa-u.ac.jp

[1] Graduate School of Engineering, Kagawa University, Takamatsu, Kagawa 761-0396, Japan

[2] Key Laboratory of Convergence Medical Engineering System and Healthcare Technology, School of Life Science and Technology, Beijing Institute of Technology, Beijing 100081, China

[3] National Rehabilitation Center for Persons with Disabilities, Tokorozawa 359-8555, Japan

[4] Faculty of Medicine, Kagawa University, Takamatsu, Kagawa 761-0793, Japan

Published online: 06 February 2023

to have real-time adaptability to the residual motor of the affected limbs for avoiding the patient–robot confrontations [16]. For the symmetric force output tasks, the output force contributions of the bilateral limbs should be kept at the same level for improving the output force control coordination ability of the bilateral limb [17]. The multi-sensory feedback is also important for hemiplegia patients to perform the bilateral isometric force control task and precept the bilateral motor skills, such as mirror visual feedback [18, 19]. In contrast, the asymmetric force output tasks are more complicated, because these tasks may require un-synchronic force outputs of the bilateral limbs to interact and compensate for each other to complete the complex bilateral force control task with good performance [20]. Especially, the bilateral asymmetric force output force would be influenced by the dynamic physical coupling condition, because one side limb will influence the coupled contralateral side limb dynamics [21]. On the other side, the kinematic coordination-based bilateral rehabilitation system may simplify the above issues by concerning the bilateral kinematic information of the dynamic bilateral task. And the kinematic trajectory of the bilateral limbs is supposed to be symmetric and synchronic in both coupled and uncoupled conditions as that can enable hemiplegia patients to perceive the natural inter-limb coordination and stimulate the re-modulation of the brain–spinal cord pathway [22]. Moreover, the compliant patient–robot interaction of bilateral rehabilitation remains challenging because the suitable robotic assistant force delivered to the affected limb is difficult to be determined when the affected limb cannot follow the desired symmetric reference trajectory as the healthy limb. The inappropriate assist force may cause potential interaction confrontation which may even lead to the training injury. Therefore, the compliant patient–robot interaction should be achieved by the safety-enhanced mechanism structure and the compliant interaction control strategy such as Assist-As-Needed (AAN) control strategy [23–25].

From the viewpoint of anatomy, human joint motion is driven by the corresponding pair of antagonistic muscles [26, 27]. Even for the same task with the same kinematic trajectory, the pair of antagonistic muscles may have different contraction levels according to the environments or task-oriented requirements (e.g., Different loads) [28]. This phenomenon is well known as the 'muscle synergy effect' [29, 30]. Moreover, the output stiffness of the joint is determined by both the variations of the pair of antagonistic muscle contraction levels and corresponding joint kinematics (such as joint position and velocity) [31]. Therefore, the synergy effect and kinematics should be investigated together for the interpretation of the specific task-oriented human motion patterns to promote the bilateral task skills transfer [32, 33]. Moreover, the muscle contractions-based synergy effects and human motor can be reflected by the electromyography (EMG) signals [11, 34]. In our previous research, we proposed a home-based variable stiffness upper limb rehabilitation system. The healthy side limb information was utilized as the reference to guide the affected side limb with tracking assistance and real-time stiffness regulation [35]. However, the compliant interaction control was ignored in this study. Recently, a novel task performance-based electromyography (EMG)-driven variable stiffness control strategy was presented, which incorporated a position-based impedance control framework for achieving the AAN–compliant interaction control, but the healthy side stiffness was transferred with the modification of the Task Performance Index (TPI), so that the affected side limb may not percept the whole stiffness profile for task skills relearning [36].

In this paper, an EMG-driven biomimetic variable stiffness modulation strategy was proposed for kinematic-based bilateral task skill relearning. A bilateral impedance control framework was implemented in the Powered Variable Stiffness Exoskeleton Device (PVSED) to adapt the proposed biomimetic variable stiffness modulation strategy for compliant patient–robot interaction. The EMG signals and kinematic trajectory of the healthy side limb were collected to generate the real-time reference stiffness profiles and reference trajectory, which will be independently reproduced by the PVSED to assist the affected side limb and facilitate task skills relearning. The contributions of this paper were summarized as follows:

1) The biomimetic variable stiffness modulation concept was proposed for upper limb elbow joint bilateral rehabilitation. By analyzing the muscle synergy effect of the healthy side limb as the reference, human motor pattern-like assistance can be achieved for the affected side limb.
2) The EMG-driven synergy reference model is utilized to construct the biomimetic variable stiffness modulation for the bilateral motor skills interpretation, which can promote bilateral motor skills relearning and bilateral inter-limb coordination.
3) The rehabilitation training safety was also enhanced by the proposed biomimetic variable stiffness modulation by incorporating the compliant mechanism VSA and the bilateral impedance control framework to achieve the compliant patient–robot interaction.

The rest of this article is organized as follows: In Section II, the overall system configuration is introduced and the biomimetic design of the PVSED is reviewed. And the proposed biomimetic variable stiffness modulation strategy is introduced in detail in Section III. Experimental results are presented in Section IV and the discussion is given in Section V. Finally, the conclusion is drawn in Section VI.

2 System Overview of the PVSED System

2.1 Mechanical Design of the PVSED

As well known, the human joint motor is mainly driven by a pair of antagonistic muscles, that can adapt to the environment for completing high-flexible and high-complexed tasks. Especially, the human upper limb is the most used during daily life activities. Regarding the elbow joint of the upper limb, it can drive the extension/flexion movements between the forearm and brachium by the pair of antagonistic muscles, the biceps, and triceps. According to the different contraction levels of the antagonistic muscles, the elbow joint can adapt to different tasks or environments from soft to hard. Inspirited by the anatomic structure of the elbow joint, a biologically inspired variable stiffness exoskeleton robot with a VSA was developed in our previous work to realize the high-adaptive independent stiffness regulation and flexible flexion/extension movements of elbow joint motor assistance for rehabilitation training [37].

The PVSED was designed in a lightweight, portable, and user-adaptive mechanical structure with one active Degree of Freedom (DOF) and 5 passive DOFs on the elbow joint. In addition, there is a VSA for active stiffness modulation of the elbow joint. The mainframe structure of the PVSED mainly includes a back frame, a shoulder frame, and an upper limb frame, as shown in Fig. 1. Each of them has an adjustable structure for adapting to the different user-specific body sizes. Moreover, there is a main joint actuator system for elbow joint flexion/extension movements and a variable stiffness actuator system for independent variable stiffness regulation. Concerning the main actuator system for achieving elbow joint flexion/extension movements, the pulley of the elbow joint is driven by a cable transmission mechanism which is connected to the DC motor (Maxon RE-30 Graphite Brushes Motor) placed on the back frame. In the independent stiffness actuator system, a VSA is implemented on the mainframe. The VSA consists of a screw with a movable pivot driven by a compact DC motor (Maxon RE-13 Graphite Brushes Motor) fixed on the mainframe, a pair of antagonistic springs, and an output link for interaction with users. If there is deflection between the mainframe and output link, the users will feel the elastic force caused by one of the antagonistic springs elongated resulting in the compliant interaction. As Fig. 2 shows, the variable stiffness principle of the PVSED can be described according to the definition of stiffness, given as

$$K = \frac{F_j \bullet l}{\theta_j - \theta_1} = \frac{F_{\text{spring}} \bullet l}{\theta_j - \theta_1} \bullet \frac{L_1}{L_2}, \tag{1}$$

where F_j represents the interaction force effecting to the output link, and F_{spring} is the spring force of the VSA. l is the moment arm of the PVSED which is a constant. The deflection angle can be calculated as $\theta_j - \theta_1$. And L_1/L_2 indicates the transmission ratio. To realize the independent variable stiffness modulation to adapt to the different tasks, the movable pivot position L_p can be controlled by the RE-13 motor rotation angle θ_2 through the ball screw, which can actively regulate the transmission ratio L_1/L_2 between the elastic element and the output link. Therefore, the desired output stiffness K of the PVSED can be realized by rotating the angle of the RE-13 motor θ_2 to change the movable pivot L_p to the corresponding position for approaching the desired transmission ratio L_1/L_2. As above analyzed, the stiffness control problem can be transferred to the RE-13 rotation control for the control practice convenience. In our previous study [38, 39], a pivot-to-stiffness identification experiment was carried out in five different pivot positions from the initial position of 0 mm to the maximal position of 20 mm with the increment of 5 mm to measure the output stiffness of the PVSED. In the trial, the output link was fixed to a force sensor (MINI 4/20, BLAUTOTEC. Ltd.), so that the force could be recorded in each position by rotating the mainframe of the PVSED. Substituting the measured force

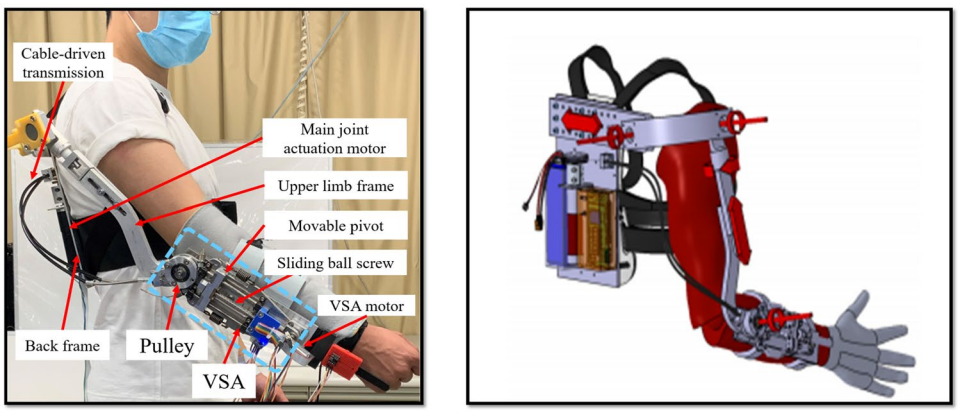

Fig. 1 Mechanical design of the PVSED. **a** Prototype of the PVSED worn by a subject. **b** Adaptive design for subject-individual body size

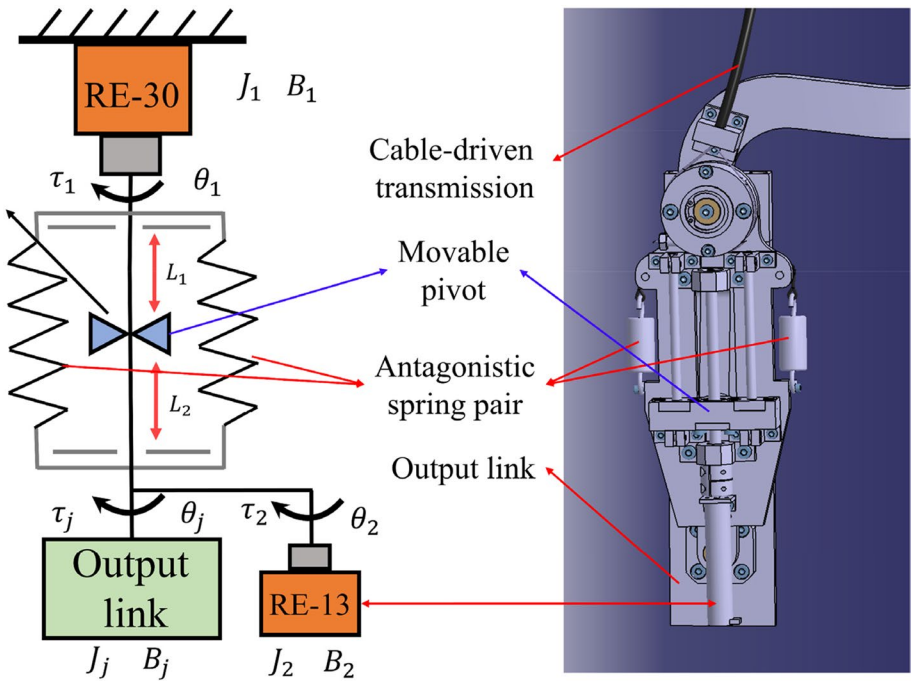

Fig. 2 Components and variable stiffness principle of the PVSED

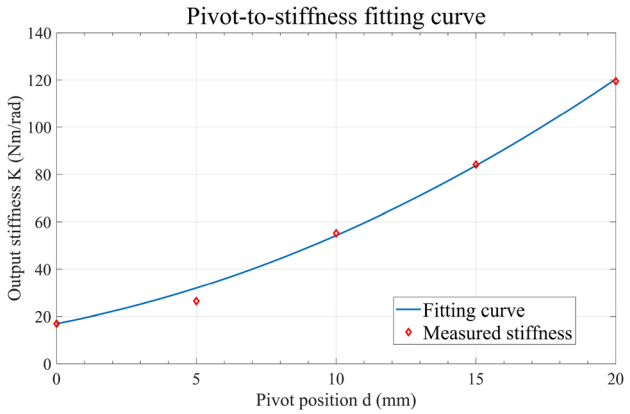

Fig. 3 Pivot-to-stiffness fitting curve

and rotation angle to Eq. 1, the output stiffness of each pivot position can be calculated and the fitting curve of pivot-to-stiffness identification could be further obtained by a least-squares-approximation-based 2nd-order polynomial fitting function as shown in Fig. 3. Therefore, the pivot-to-stiffness identification function is described as follows:

$$K(\theta_2) = 0.1443L_p(\theta_2)^2 + 2.287L_p(\theta_2) + 16.95\left(0 < L_p(\theta_2) < 20\text{mm}\right), \tag{2}$$

where the K represents the output stiffness of the PVSED. And the θ_2 stands for the rotation angle of the RE-13 motor of the VSA. And $L_p(\theta_2)$ is the pivot position. Therefore, the output stiffness can be calculated by Eq. 2 only using the RE-13 rotation, which can be used in practice for independent variable stiffness regulation. It should be noted that the pivot position has a constant range according to the ball screw length, which means that the output K is also bounded. From the pivot-to-stiffness identification experiment results, the minimal output stiffness $K_{\min}$ and the maximal output stiffness $K_{\max}$ of the PVSED are 16.95 Nm/rad and 119.5 Nm/rad, respectively. Benefiting from this human joint-like biomimetic design, the PVSED can provide highly flexible and compliant motor assistance on the elbow joint of the patient.

2.2 Control System Setup

Bilateral rehabilitation utilizes simultaneous and symmetric bimanual motor tasks in which the hemiplegia patients were instructed to simultaneously perform the training task by both their health side and affected side limb to promote the natural coordination of bilateral limbs. Significantly, the biomechanical information of the healthy side limb is the most meaningful reference for the affected side limb during this bilateral symmetric and synchronic rehabilitation training task. Therefore, both the kinematic trajectory and dynamic profile of bilateral limbs should be considered together. For this purpose, the bilateral rehabilitation system should enable symmetric motion tracking assistance and enable hemiplegia patients to percept the dynamic contralateral biomechanical reference information for facilitating the bilateral motor skill transfer. In this study, the overall system configuration is designed for achieving trajectory tracking and independent stiffness modulation, including the processor unit, motor sensory unit of healthy side motion capture,

PVSED kinematic sensory units, EMG signals collection and processing unit, and the PVSED motor control unit, as Fig. 4 shown. The Arduino mega 2560 was selected as the processor unit to communicate each sensor and control the servo motor controller for motor trajectory tracking control and to implement the EMG-driven synergy reference stiffness estimation model. For the trajectory tracking control, there is an inertial measurement unit (GY-25 T tilt angle module) placed on the healthy side limb to capture the reference trajectory of the bilateral training task. And the other two were attached to the output link of the PVSED coupled with the affected side limb to collect the actual position, and the main frame of the PVSED for calculating the deflection of the VSA, respectively. Each of the inertial measurement units communicates with the processor unit by the I^2C method. In the PVSED motor control unit, two ESCON 50/5 servo controllers were employed to drive the DC motor RE-30 of the main joint actuator system and RE-13 of the variable stiffness actuator system by the PWM command from the processor unit. In the stiffness modulation system, the desired rotation angle of the RE-13 motor can be derived by the desired output stiffness according to Eq. 2, and a PID controller was implemented to drive the RE-13 motor for high-precision angle rotation control. To realize the compliant pHRI under the variable stiffness, a hierarchical compliant assistance tracking controller was implemented in the main actuator system to control the RE-30 motor for bilateral limbs' kinematic coordination and to avoid patient–robot confrontation, which will be introduced in Sect. 3.3. As above introduced, the proposed control system can capture the kinematic trajectory of bilateral limbs and the EMG signals of the healthy side limb to control the joint movement and stiffness of the PVSED to provide bilateral motor assistance for symmetric mirror motor perception and independent stiffness regulation for adjustable training intensities and high subject-adaptability.

3 Motor Skills Relearning-Oriented Biomimetic Stiffness Modulation Strategy

In this section, the technical details of the proposed EMG-based biomimetic stiffness modulation strategy will be introduced for bilateral motor skills relearning. First, the EMG signals from the healthy side limb will be collected and processed for calculating muscle activation. Then, the muscle synergy reference model was utilized to estimate the reference stiffness using the obtained muscle activations. The overall computational produce of the EMG signals is shown in Fig. 5. Finally, a biomimetic impedance controller cascaded with an inverse dynamic-based torque controller was implemented for realizing the bilateral motor skill relearning-oriented stiffness modulation and bilateral symmetric motion tracking.

3.1 EMG Signal Collection and Preprocessing

Along with the muscle fiber's contraction driven by the neural impulses, there will be an electronic potential difference on the muscle fiber sides. Therefore, the muscle activation dynamics can be quantitatively represented through the EMG signals that are the sum of this muscle fiber electronic potentials. For single muscle activation, the raw EMG signals can be collected by an electrode placed on the specific position of the muscle. In this study, the commercial EMG device (Personal-EMG. Oisaka Electronic Equipment Ltd, Japan) was utilized for collecting the raw EMG signals at a 1000 Hz sampling rate. Due to the noise always exists

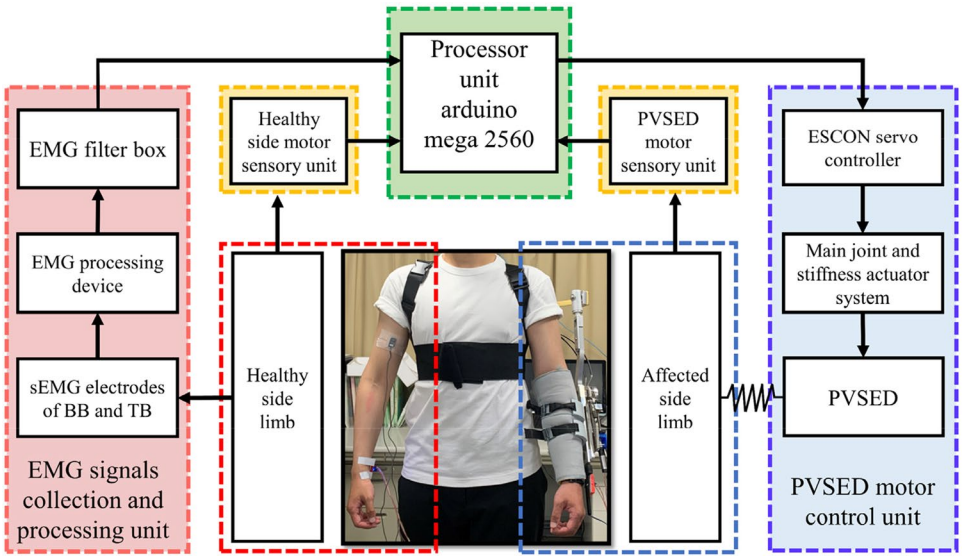

Fig. 4 Control system configuration diagram

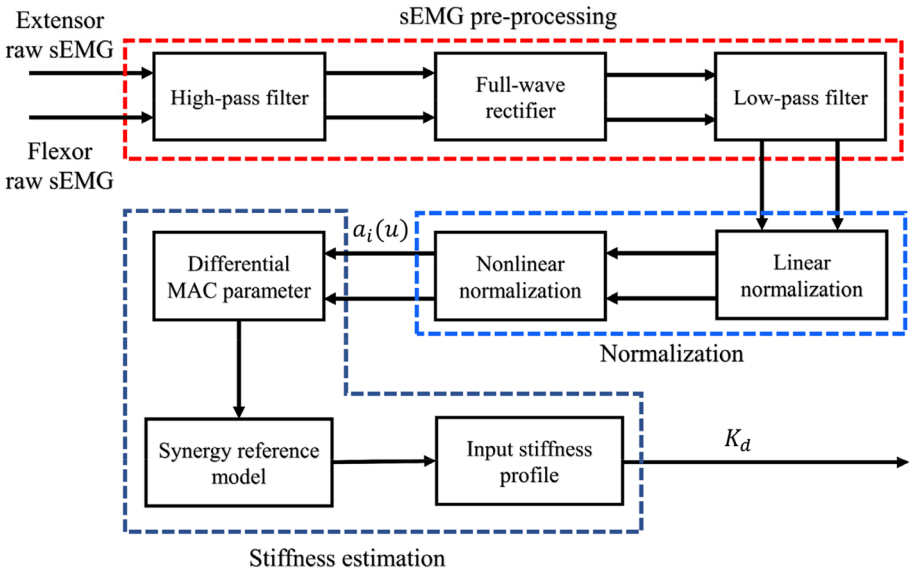

Fig. 5 Computational produce of the EMG signals from the biceps and triceps

during the signal sampling processing, the raw EMG signals should be filtered for noise rejection by the EMG signal filter (Personal-EMG filter box, Oisaka Electronic Equipment Ltd, Japan). After noise rejection, the EMG signals should be processed for normalization. A fourth-order Butterworth high-pass filter with a cut-off frequency 10 Hz, a full-wave rectifier, and a low-pass filter with a cut-off frequency 2 Hz was used to get the filtered EMG signals. In the normalization processing, the linear normalized EMG was calculated from the Maximum Voluntary Contraction (MVC) test at first, and a nonlinear normalization was applied to transfer the Muscle Activation Level (MAL) as follows:

$$A_i(u) = \frac{e^{an_i} - 1}{e^a - 1}, \tag{3}$$

where n stands for the processed EMG signals and a is a nonlinear shape factor and was selected as -0.1 in this study.

3.2 Synergy Reference Stiffness Estimation Model

The human motor patterns can be represented as the synergy effect by the corresponding muscles' contractions. Moreover, the muscle synergy effects can reflect the specific task skills and the subject-specific motor preference. Even for the same task, the preference of different subjects will lead to differences in the muscle synergy patterns. Therefore, for hemiplegia patients, the synergy effect of healthy side limbs was utilized as the symmetric and synchronic reference for realizing the bilateral motor skills relearning in this study.

To illustrate the synergy effect of bilateral motor tasks, the motor behaviors are decomposed into two parts in this paper, including the kinematic metric and dynamic metric. Regarding the kinematic metric, the limb movement trajectory in task space provides the basic evaluation of the symmetry and synchronization of the motor task, which should be symmetric with the middle line of the subject body. Furthermore, the task intensity, environmental load, and the participant level of the subjects, which reflect the dynamic characteristic, are considered the dynamic metric in this study. For the flexion/extension motion of the upper limb elbow joint, the extension motion in the sagittal plane is generated by biceps contracting and triceps relaxing, and vice versa. The muscle stiffness is also dynamically variable along with the contraction and relaxation, which can be reflected by the EMG signals, shown in Fig. 6. To establish the relationship between the EMG signals and force/stiffness characteristics, an antagonistic effect-based model was utilized as the reference [40]. As the effect of a pair of antagonistic muscles, the joint output torque τ and the joint output reference stiffness K_r generated by the muscular contraction flexors and extensors can be represented as follows:

$$\tau = a_\tau \bullet \delta\left(A_f, A_e\right) \tag{4}$$

$$K_r = a_k \bullet K_s\left(A_f, A_e\right), \tag{5}$$

where a_τ is the torque transfer gain and a_k represents the stiffness transfer gain. The A_f and A_e are the MAL of flexors and extensors. The $\delta(\bullet)$ is the MAL difference of the antagonistic muscles referring to $A_f - A_e$. In addition, the stiffness parameter function $K_s(\bullet)$ is determined by the combination of the muscle activation levels of antagonistic muscles $A_f + A_e$. The definition of the $\delta(\bullet)$ and $k_s(\bullet)$ is given by the hyperbolic tangent functions as follows:

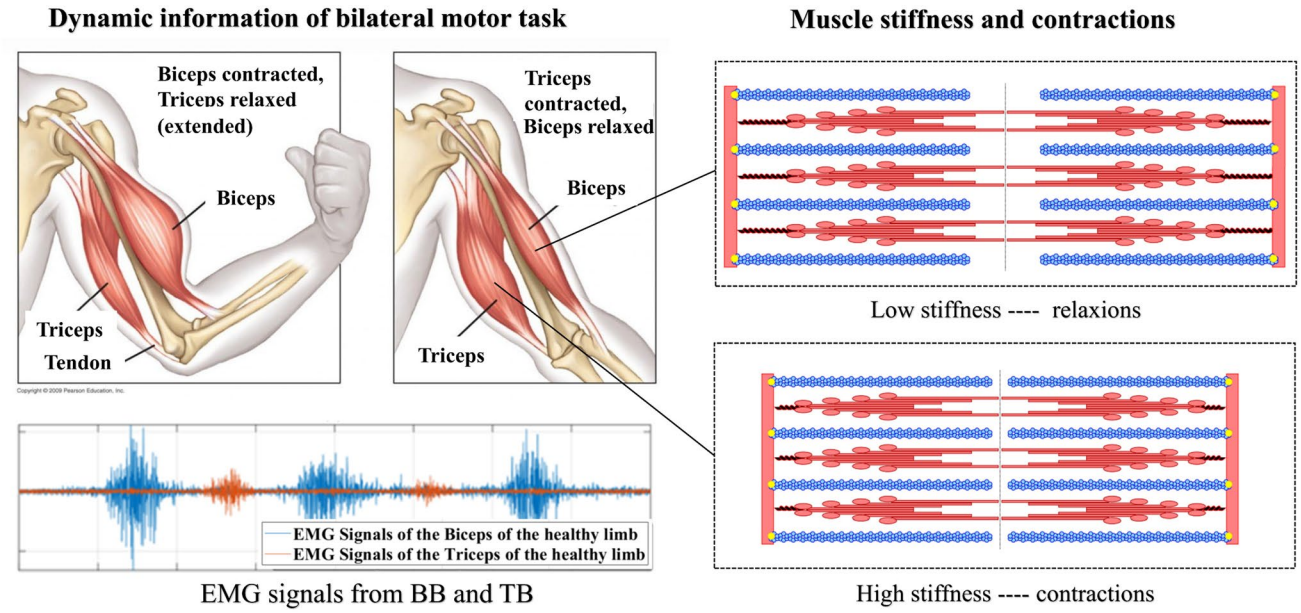

Fig. 6 The synergy effect of the biceps and triceps during the flexion/extension motion of the elbow joint in sagittal plane (Picture reference by http://gymlion.com/what-are-the-best-tricep-exercises/ and https://imgbin.com/png/9QzZSDxg/sliding-filament-theory-muscle-contraction-myosin-sarcomere-myofilament-png)

$$\delta\left(A_f, A_e\right) = \frac{a_\delta \bullet \left(1 - e^{-b_\delta\left(A_f - A_e\right)}\right)}{1 + e^{-b_\delta\left(A_f - A_e\right)}} \tag{6}$$

$$K_s\left(A_f, A_e\right) = \frac{a_k \bullet \left(1 - e^{-b_k\left(A_f + A_e\right)}\right)}{1 + e^{-b_k\left(A_f + A_e\right)}}, \tag{7}$$

where a_δ, b_δ, a_k, and b_k are the positive constant gains that can be obtained by a calibration experiment. As the reference stiffness K_r of the healthy side limb has been obtained, the PVSED should reproduce this dynamic joint stiffness in the affected side limb for motor task skills transfer. Therefore, the mapping relationship between the healthy side reference joint stiffness K_r and the desired PVSED stiffness K_d should be established. Considering the variable stiffness range of the PVSED, the desired stiffness of the VSA can be calculated by the following linear mapping function:

$$K_d = K_r\left(K_{\max} - K_{\min}\right) + K_{\min}, \tag{8}$$

where the $K_{\max}$ is 119.5Nm/rad and $K_{\min}$ is 16.95Nm/rad as introduced in Sect. 2.1. And K_r is the reference stiffness of healthy side limb obtained by the EMG-driven synergy reference stiffness estimation model. All the computational produce was implemented in the processor unit. Benefiting from this synergy reference model, the dynamic reference metric of the bilateral task can be quantitatively calculated only using the muscle activation levels of the pair of antagonistic muscles.

3.3 Bilateral Impedance Control

To avoid the potential patient–robot confrontations for training safety, the impedance control strategy was implemented to deliberately regulate the desired delicate soft compliant assistive behaviors to provide compliant physical human–robot interaction. Significantly, the motivation of the proposed bilateral impedance control is to transfer the dynamic reference biomechanical characteristics from the healthy side limb to the affected side limb for promoting the bilateral motor task skills, shown in Fig. 7. For this purpose, the bilateral impedance control is given as follows:

$$M_h\left(\ddot{\theta}_j - \ddot{\theta}_h\right) + B_h\left(\dot{\theta}_j - \dot{\theta}_h\right) + K_h\left(\theta_j - \theta_h\right) = \tau_j, \tag{9}$$

where θ_h, and its first- and second-order derivation, are the angular position, velocity, and acceleration of the healthy side limb. Similarly, θ_j, and its first- and second-order derivation, are the angular position, velocity, and acceleration of the output link, which also can refer to the affected side limb. And the M_h, B_h, and K_h are the inertia, damping, and stiffness parameter of the healthy side limb, which are expected to be transferred to the affected side limb. Due to the subject-specific body size and mass, the biomechanical parameters should be measured and calculated in advance as follows [41]:

$$M_h = \frac{2}{3} m_f \bullet l_f^2 \tag{10}$$

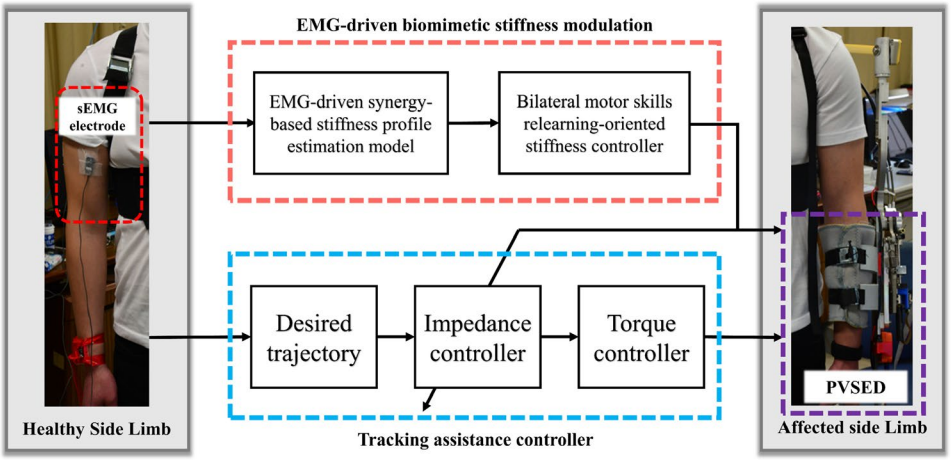

Fig. 7 Control framework

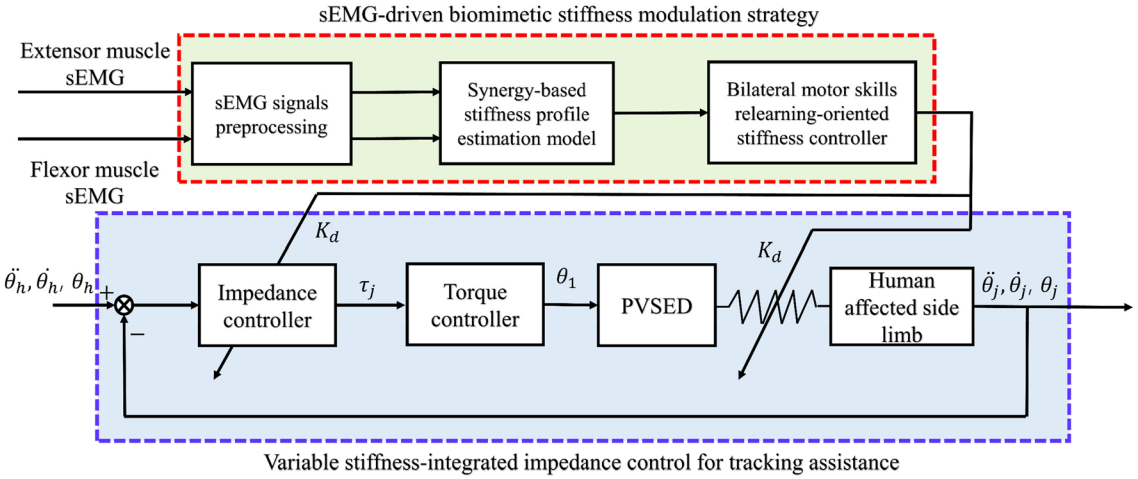

Fig. 8 Control block diagram

$$K_h = K_d \tag{11}$$

$$B_h = v_m\sqrt{K_h}, \tag{12}$$

where m_f and l_f are the mass of the human forearm and length from the center of the forearm to the elbow joint. And v_m stands for the damping coefficient, which is set at 0.7. By incorporating the estimated stiffness from the synergy reference model as Eq. 10, the biomechanical impedance characteristics can be transferred to the affected side limb including the real-time varying stiffness and damping features. The output of the bilateral impedance control is the desired torque to control the main actuator system of the PVSED. Considering the human–robot coupled system, the coupled dynamics can be described as follows:

$$M_j\ddot{\theta}_j + B_j\dot{\theta}_j + G_j = \tau_j + u \tag{13}$$

$$\tau_j = K(\theta_2) \bullet (\theta_1 - \theta_j), \tag{14}$$

where M_j, B_j, and G_j are the inertia, damping, and gravitational term of the human–robot coupled system mass of the human forearm and length from the center of the forearm to the elbow joint. τ_j is the torque generated from the VSA calculated as Eq. 14. Due to the active participation of the subjects, the coupled dynamics can be adaptively offset by the human voluntary motion [42]. According to the certainly equivalent principle, the control effort u can be derived from Eq. 12 by inverse dynamics as

$$u = \widehat{M}_j\left(\ddot{\theta}_h - \frac{B_h}{M_h}(\dot{\theta}_j - \dot{\theta}_h) - \frac{K_h}{M_h}(\theta_j - \theta_h) - \frac{1}{M_h}\hat{\tau}_j\right) + \hat{B}_j\dot{\theta}_j + \hat{G}_j - \hat{\tau}_j. \tag{15}$$

The overall control framework is summarized in Fig. 8. In practice, the desired kinematic trajectory of the healthy side and the actual position of the PVSED can be captured by the GY-25 T IMU sensor and transferred to the processor unit.

Moreover, the filtered EMG signals can be recorded and calculated as the synergy-based reference stiffness estimation model to obtain the input stiffness K_h and damping B_h by the processor unit. For realizing the real-time independent stiffness modulation, the input stiffness K_h can be transferred to the desired rotation angle of the variable stiffness actuator system as Eq. 2. For achieving the compliant tracking assistance control, the desired control input u of the PVSED can be derived according to Eqs. 9 and 15.

To sum up, the dynamic reference metric was estimated by the synergy reference model introduced in Sect. 3.2, which was utilized to real-time regulate and transfer the bilateral biomechanical impedance characteristics from the healthy side limb to the affected side limb for promoting bilateral skill relearning. The bilateral impedance controller cascaded with an inverse dynamics-based torque controller was implemented to realize compliant assistance control for the human–robot coupled system shown in Fig. 9. Furthermore, when the affected side limb could not complete the desired task trajectory as the healthy side limb, the robot would provide a compliant assistance force to the affected limb by the VSA according to the proposed EMG-driven stiffness modulation strategy and bilateral impedance controller. Once patients feel uncomfortable on the affected limb, patients can actively relax their healthy side limb muscle, which can reduce the PVSED stiffness and damping and further decrease the interaction force as Eq. 9 shown. Therefore, the proposed control framework can intuitively enhance patient–robot interaction safety by the passive compliant mechanism VSA and active myoelectric variable stiffness control.

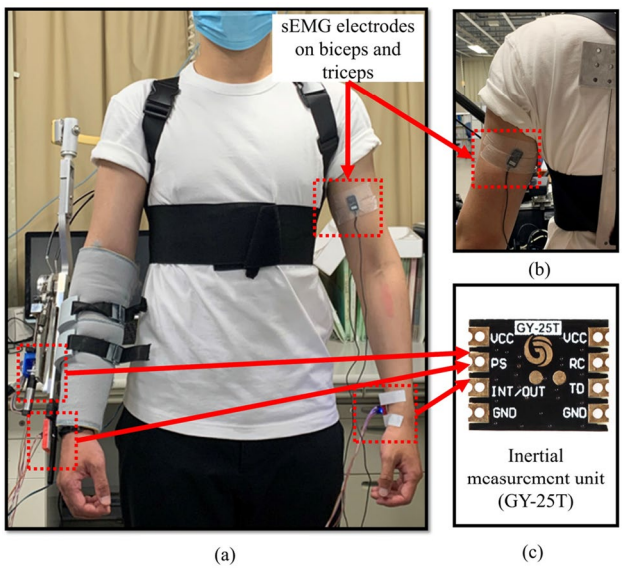

Fig. 9 Experiment setup

4 Experiments

4.1 Experimental Protocols

In this study, the symmetric bilateral curl movements of the elbow joint flexion/extension were selected as the bilateral motor task. The subjects were instructed to stand in front of the monitor and wear the PVSED on their right-side limb, which was considered the affected side in this study. After skin cleaning by alcohol for rejecting skin bioimpedance disturb, two Ag/AgCl dry electrodes were attached to the biceps and triceps of the contralateral side limb for raw EMG signals' collections. And the overall system was set up as Sect. 2.2 introduced to realize the proposed biomimetic stiffness modulation strategy. During the experiment, the subjects were asked to naturally perform the bilateral curl motor task. At the same time, the raw EMG signals of the healthy limb, and kinematic information of both side limbs were recorded for stiffness estimation and assistive interaction control. All the experiment setups are shown in Fig. 9. Due to the rehabilitation intensity should be adjustable for different recovery stage patients, we also explored the different task intensity influences on bilateral motor skills relearning for the middle or last recovery stage. This experimental protocol would be reproduced with 1.5 kg load and 2.5 kg load using dumbbells according to [43] suggested. Five healthy volunteers (male, 25 ± 3 years old, 172 ± 4 cm, 65 ± 10.2 kg) were recruited for this study. No subject had any neuromuscular disorder history. And all subjects have been well understood and agreed with the experiment protocols with signed consent. All the experimental protocols were admitted by the Institutional Review Board (IRB) in the Faculty of Engineering, Kagawa University (Ref. No. 01–110).

4.2 Experimental Results

To validate the performance of the proposed biomimetic stiffness modulation strategy, first, we conducted a compassion experiment between the low/high stiffness condition without biomimetic variable stiffness and biomimetic variable stiffness condition. Considering the variable range of the PVSED introduced as Sect. 2.1, the minimal stiffness $K_{\min}$ 16.95 Nm/rad was set as a low stiffness condition and maximal stiffness $K_{\max}$ 119.5 Nm/rad was selected as a high stiffness condition. As Fig. 10 shows, there is an increasing trend in the tracking error from the low stiffness condition to the high stiffness condition which is also corresponding to the increasing trend of the stiffness. This phenomenon is consistent with our previous study, because as the stiffness increases, the torque to generate the same deviation angle of the VSA is also increasing. Therefore, the interaction

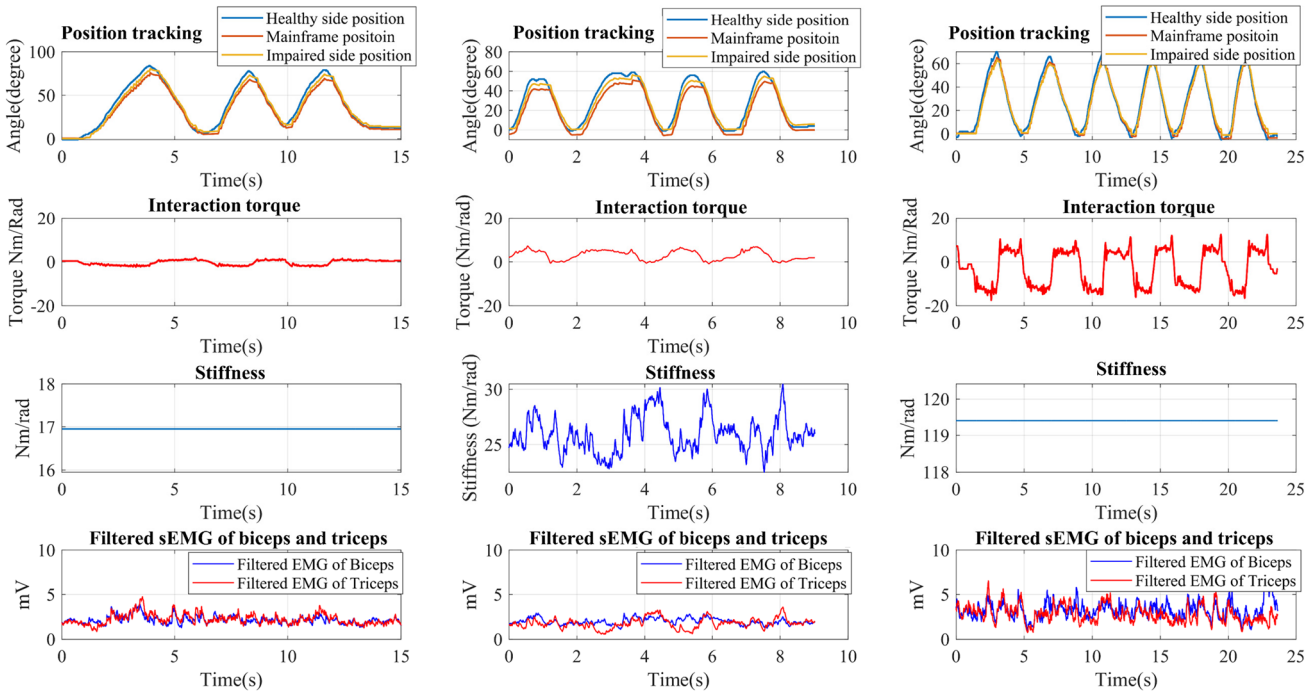

Fig. 10 Comparison results of low stiffness condition, biomimetic variable stiffness condition, and high stiffness condition. **a** Low stiffness without biomimetic variable stiffness. **b** Biomimetic variable stiffness. **c** High stiffness without biomimetic variable stiffness

torque, related to the deviation angle and the stiffness of the VSA, also conforms to this phenomenon. The interaction torques of low stiffness and high stiffness conditions are only related to the deviation angle due to the constant stiffness set due to the EMG-based biomimetic stiffness modulation strategy are not incorporated. In the biomimetic variable stiffness condition, the PVSED output stiffness could influence the interaction torque according to the desired stiffness calculated from the healthy side EMG signals that can validate the feasibility of the proposed biomimetic stiffness modulation strategy. Furthermore, we found that the peak interaction torques of every curl movement are different in biomimetic variable stiffness condition, which indicated that the dynamic bilateral motor skills were reproduced by the PVSED and precepted by the affected limb. Compared to the constant stiffness condition, the biomimetic variable stiffness is more suitable for bilateral rehabilitation as it can provide more individual-adaptive training reference according to the dynamic biomechanical information of the healthy side for promoting inter-limb coordination.

To further evaluate the performance of the rendering of a wide range of human motor patterns of the proposed biomimetic stiffness modulation strategy, a different load condition comparison experiment was conducted too with 0, 1.5, and 2.5 kg load conditions. In the 0 kg condition as Fig. 11, the amplitudes of the EMG signals from the BB and TB were under 4 mV, which refers to the natural curl movements of the elbow joint flexion/extension. As the proposed biomimetic stiffness modulation strategy, the desired stiffness and damping profile were under the maximal values 30Nm/rad and 4Nm/rad for all 5 subjects. However, due to the subject-individual task performance, the average tracking errors of 5 subjects have no relationship which leads to the not significant relationship between the average torques of 5 subjects too. On the other hand, a strong relationship could be found for the single subject condition that the average torques were determined by the deviation angles of the training task. Generally, the stiffness and damping profiles were regulated according to the EMG signals from the contralateral side limb in real time, and the coordination of the bilateral limbs can be achieved. All 5 subject condition confirms this phenomenon. For the 1.5 kg load condition as Fig. 12, the amplitude of the EMG signals increased obviously, which also led to the increase of the desired stiffness and damping profiles. Different from the 0 kg load condition, the average torques were related to both tracking performance and desired stiffness profile, which can be attributed to the relatively large stiffness caused by the larger EMG signal amplitude. Similar to the 0 kg load condition, all 5 subjects could perform the bilateral curl movements with the 1.5 kg load. For the 2.5 kg load condition as Fig. 13, due to the further increased load, the amplitude of the EMG signals got large too. Meanwhile, the desired stiffness and damping profiles came as the relatively largest among the three load conditions. Similar to the 1.5 kg condition, the average torque was also related to both task performance and

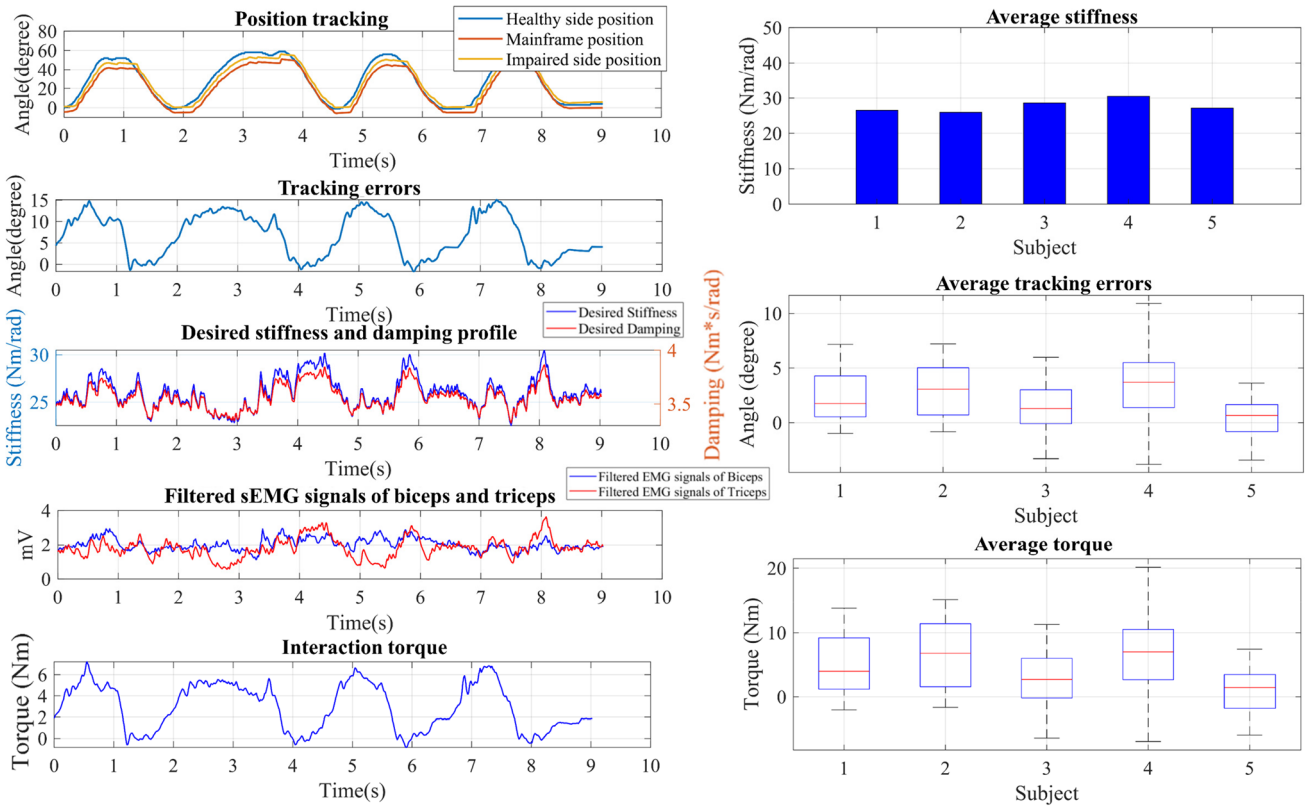

Fig. 11 Experimental results of 0 kg condition

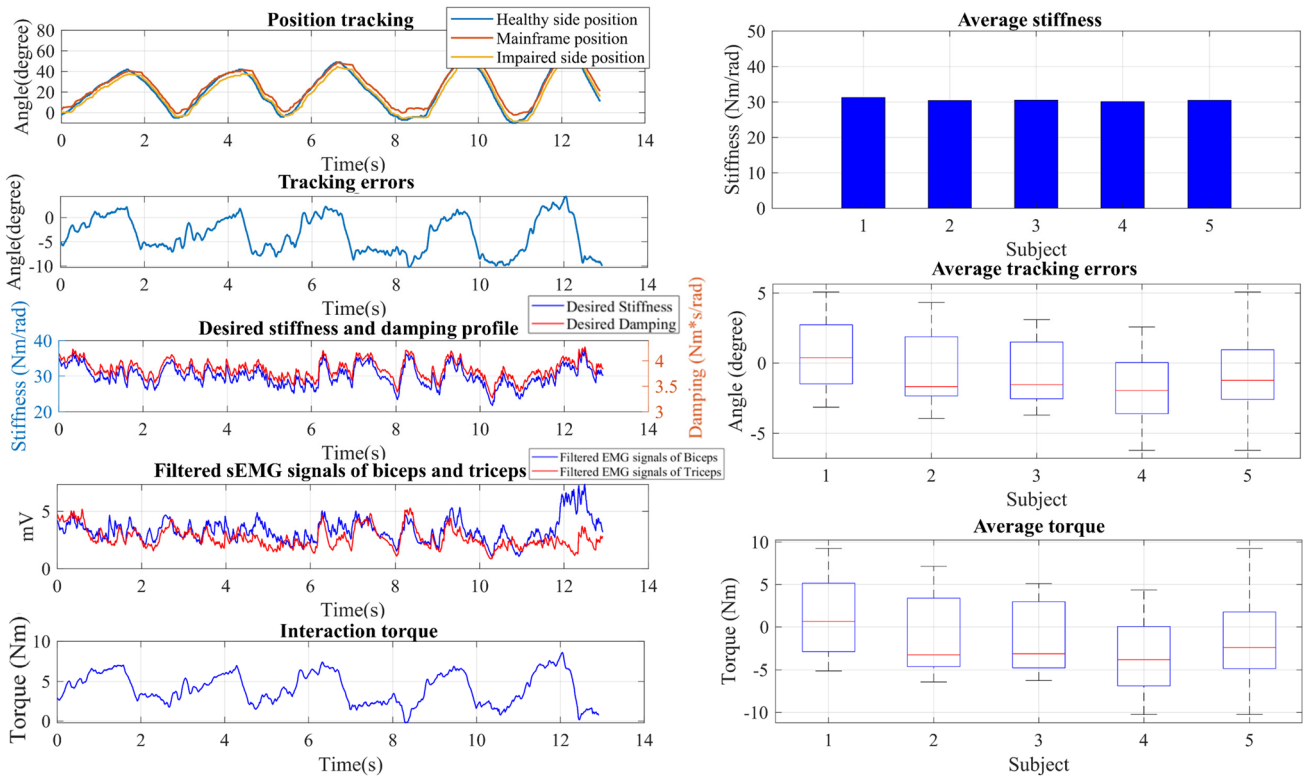

Fig. 12 Experimental results of 1.5 kg condition

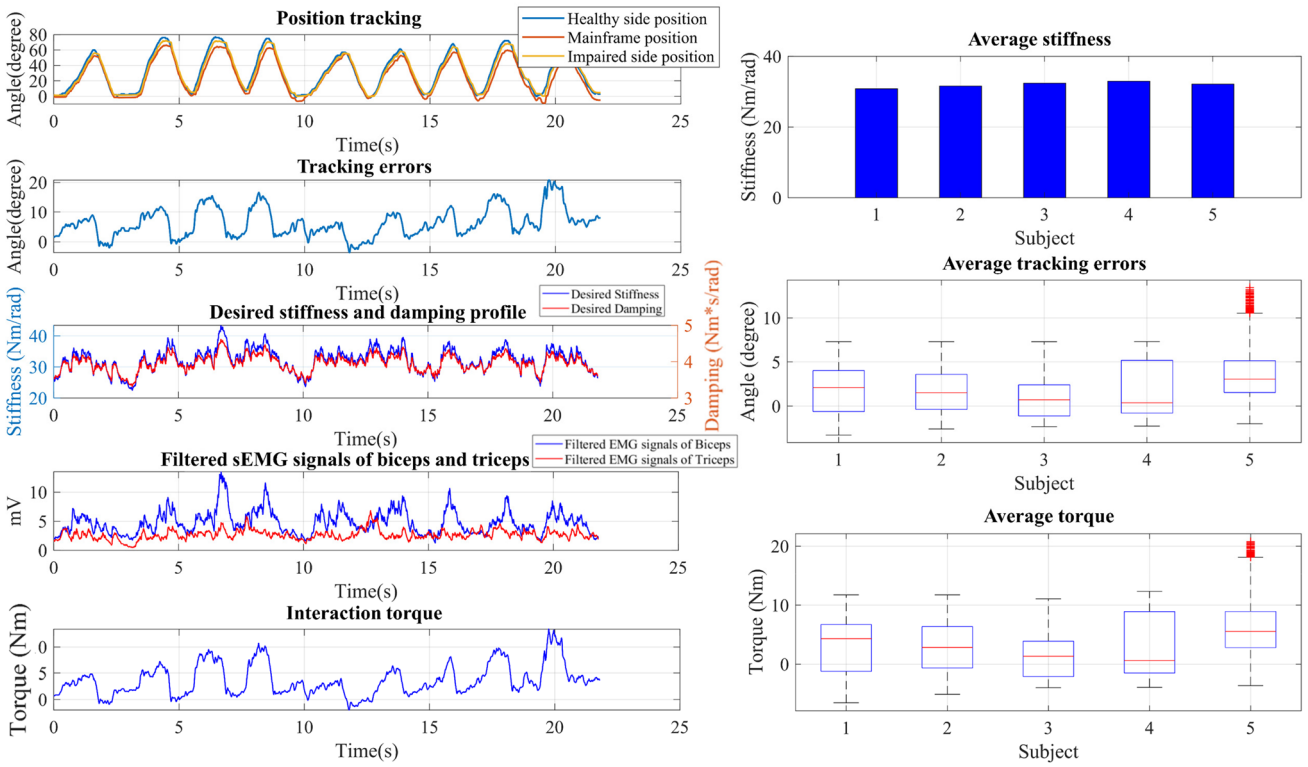

Fig. 13 Experimental results of 2.5 kg condition

desired stiffness profiles. This reason was the same due to the increased EMG signals causing a large desired stiffness profile. It should be noted that there were some abnormal values in the average tracking error and average torque in the No.5 subject trials. That may cause by the relatively large load leading to the extreme difficulty to conduct good task performance for this subject, which results in abnormal values in the average tracking errors. Furthermore, due to the torque generated by the deviation angle and desired stiffness, abnormal torque values were conducted.

5 Discussion

The robotic-aided bilateral rehabilitation training is a promising approach to recovering the bilateral limb coordination of hemiplegia patients. Regarding the mirror bilateral training task, the bilateral limb kinematic trajectories are expected to be exactly symmetric, which requires the rehabilitation robot system can assist the affected side limb to track the desired trajectory of the healthy side limb in a proper means. Because of the weakness of the affected side limb, the patient–robot interaction assistance is supposed to be compliant and flexible to enhance training safety. Especially for the exoskeleton-type rehabilitation robotic system, the patient's affected limb is usually fixed on the exoskeleton robot which leads to the coupled patient–robot interaction system. In this study, the passive compliance was enabled by the variable stiffness exoskeleton robot PVSED which integrates an antagonistic-based VSA in the forearm to actively adjust the output stiffness of the elbow joint. The performance and advantages of the PVSED have been evaluated in our previous studies [35]. As Fig. 10 shows, the average interaction torques of the minimal stiffness level 16.95 Nm/rad to the maximal stiffness level 119.5 Nm/rad varied from 0.36 Nm to 3.05 Nm. As the independent variable stiffness modulation of the PVSED, the different output stiffness levels could bring the different compliant characteristics of the patient–robot interaction for patients of different injury levels or different recovery stages.

In addition, the VSA-integrated robot can contribute to the adaptability of a wide range of task intensity and difficulty. When humans perform the upper limb bilateral motor tasks, the pair of the antagonistic muscles on the corresponding joint could actively adjust the contraction level to generate the optimal joint output torque and stiffness for adapting to the different task requirements. This cooperation of the antagonistic muscles represents the motor synergy effect which can be considered as an interpretation of the bilateral motor pattern and skills. To quantitatively calculate and reproduce the desired motor pattern and skills of the bilateral mirror motor task, an EMG-driven synergy reference

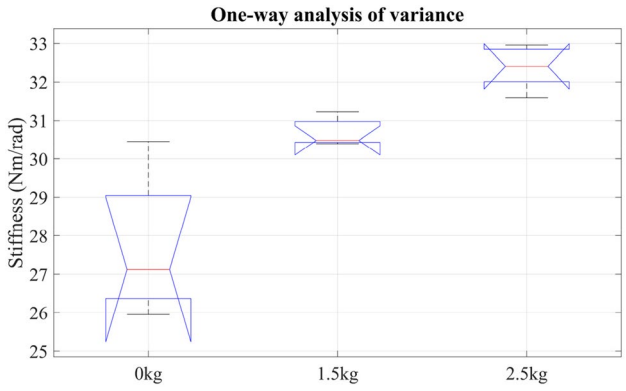

Fig. 14 One-way analysis of variance results of three load conditions

Table 1 ANOVA results

Source	SS	DF	MS	*F*	*P* value
0 kg, 1.5 kg, 2.5 kg	55.6386	2	27.8193	22.41	$8.8785 \times 10-5$
Error	14.8984	12	1.2415		
Total	70.537	14			

stiffness estimation model was implemented in this study by which the torque and stiffness profiles of the healthy side limb could be obtained in real time. The EMG signals of the antagonistic flexors and extensors (biceps and triceps in this study) were collected during the bilateral training tasks. After the noise rejection and preprocessing, the filtered EMG signals were utilized to obtain the muscle contraction level for calculating the desired joint output torque and stiffness. To illustrate the muscle synergy effect on the different task intensities and difficulties, a comparison experiment was conducted with 0, 1.5, and 2.5 kg load conditions. From the experimental results, the amplitudes of the EMG signals increased from 2.252 to 4.607 mV for biceps and 2.629 to 3.0107 mV for triceps according to the 0–2.5 kg load conditions, which is caused by the EMG signal is always positive correlative with the muscle output force. Due to this reason, the desired stiffness profiles calculated by the synergy reference model in three load conditions were also increased from 27.759Nm/rad in 0 kg, 30.459Nm/rad in 1.5 kg to 32.981Nm/rad in 2.5 kg. For the real-time task performance, the desired stiffness could be exactly reproduced by the VSA for all load conditions of all 5 subjects as shown in Figs. 11, 12, 13. Furthermore, a one-way Analysis of Variance (ANOVA) was conducted, as Fig. 14 shown. And the p-value is 8.8785×10^{-5} that indicates the differences between the stiffness of the three load condition means are significant, shown in Table 1. Therefore, the proposed EMG-based synergy reference model could quantitatively represent the different bilateral motor skills by the output stiffness transfer. Employing the reference stiffness transfer, the affected side limb could precept the task-specific output stiffness under the reference guidance of the healthy side limb. These task-specific output stiffness profiles from the healthy side limb are the most optimal for hemiplegia patients, because it represents their individual-specific motor skills for completing and adapting to the wide-range intensities of bilateral mirror synchronic task.

As above discussed, the proposed biomimetic variable stiffness modulation strategy could independently regulate the PVSED output stiffness for the patient–robot coupled interaction system. Due to the variable stiffness characteristic of the overall system, the system impedance characteristic should be consistent with the variable stiffness profiles. For this purpose, the damping level of the coupled system was also set as a dynamic variable corresponding to the variable stiffness as Eq. 12. From the experimental results, it is obvious that the damping profiles were consistent with the desired stiffness profiles for achieving the system output impedance level adjustment as Fig. 11, 12, 13 shown. It should be noted that the motivation for implementing the bilateral impedance control is aiming to provide active compliance to the coupled patient–robot interaction system, because impedance control could allow bad task performance (tracking errors) and generate compliant force feedback to correct the tracking errors. Furthermore, by incorporating the bilateral impedance control, the damping item could bring extra force to stabilize the oscillation caused by the stiffness term for further enhancing the safety of the patient–robot interactions, and the patient can intuitively control the stiffness of the PVSED by the contractions of the muscles for active training intensity self-adjustment. Meanwhile, the tracking performance could be further improved by this damping effect, which can be proved from the experimental results that the average tracking errors of 0, 1.5, and 2.5 kg were 4.96 degrees, 4.06 degrees, and 2.77 degrees and the average dampings are 3.68 Nm • s/rad, 3.85 Nm • s/rad, and 3.95 Nm • s/rad, which indicated that the tracking errors were eliminated by the increasing damping coefficient. Noted that the results of subject 5 in the 2.5 kg condition were excluded, because there were abnormal values of the tracking errors due to the inadequate motor ability to 2.5 kg load. These results also reveal that all 5 subjects could perform the bilateral curl task for all load conditions with the aid of the proposed biomimetic variable stiffness modulation system. To sum up, the experimental results evidenced that the proposed biomimetic stiffness modulation strategy has the ability to reproduce the bilateral motor pattern and skills by means of variable stiffness for promoting the motor ability relearning of hemiplegia patients.

Although the advantages of the proposed system have been shown, there are still some limitations in this study. First, the total dynamics of the human upper limb and the PVSED were considered for representing the patient–robot coupled system. However, some uncertain terms of the system dynamics and the limited precision of the dynamic identification are still existing. In this study, we ignored the influence caused by system uncertain dynamics and only the inverse dynamic-based control framework was realized for a feasibility study, which is expected to be improved in future works. Second, as mentioned above, there were abnormal values in the experimental trials of subject 5 in the 2.5 kg load condition. The reason for this issue is the inadequate motor ability of subject 5 within the 2.5 kg condition. From this phenomenon, the proposed biomimetic variable stiffness modulation strategy could only be efficient only if the subjects have the ability on completing the training task. Therefore, we argue that the proposed biomimetic variable stiffness modulation strategy is limited by the motor ability of the subjects, which indicated that the proposed system could assist hemiplegia patients in regaining the motor ability of their healthy side limb rather than augmenting the motor ability more than themselves. Third, only the bilateral elbow flexion/extension motion task was validated in this study. Because there is only one active DOF on the elbow joint of the PVSED, this paper focuses on the feasibility validation of the proposed biomimetic variable stiffness control strategy which can adapt to the bilateral motor task intensities and individual-specific by independent joint motion control and stiffness regulation. However, the proposed control strategy is expected to be applied to multi-DOF variable stiffness robots. In the multi-DOF condition, we should determine the stiffness matrix of the target muscle synergy effects corresponding joints and regulate them independently. Moreover, the human–robot coupled system dynamic and bilateral impedance control should also be transferred to the matrix form for adapting the multi-DOF condition. The multi-DOF condition will be validated in the developed multi-DOF PVSED in our future work. Fourth, only healthy subjects were involved in this research for preliminary evaluation of the proposed method. Clinical trials with hemiplegia patients are expected to be conducted for further evaluation. Therefore, the challenges of the clinical application also should be noted. The synergy reference model should be calibrated in advance for obtaining the precisive model parameters. Although this synergy reference model is relatively simple than the hill-model-based musculoskeletal model, the parameter calibration is still time-consuming. Furthermore, the predefined bilateral training tasks should also be adjusted according to the therapist for different injury level patients (for example, the training motion ranges should be adaptive to patients' disable states).

6 Conclusion

This paper presented a novel EMG-driven biomimetic variable stiffness modulation strategy that incorporates the bilateral impedance control framework aiming to promote bilateral motor skills relearning for hemiplegia patients. Preliminary experiments were carried out to evaluate the feasibility and performance of the proposed variable stiffness rehabilitation strategy. The different load experiments reveal that the proposed strategy could transfer the wide-range bilateral motor patterns and skills of the healthy side limb to the affected side limb within the different task intensities. The proposed biomimetic stiffness modulation strategy has the following advantages:

1) The biomimetic variable stiffness modulation concept was proposed for upper limb elbow joint rehabilitation, which is aiming to promote inter-limb coordination and bilateral motor skill relearning. The bilateral motor skills were interpreted by the synergy effect of the pair of antagonistic muscles on the elbow joint using the EMG-based synergy reference stiffness estimation model.
2) Benefiting from the proposed synergy reference model, the bilateral motor patterns and task skills could be quantitatively represented by the EMG signals from the specified antagonistic muscles on the joint. Furthermore, as the comparison experimental results of the different loads show that the average stiffness values are 27.759 Nm/rad in 0 kg, 30.459 Nm/rad in 1.5 kg to 32.981 Nm/rad in 2.5 kg, respectively, the affected side limb could percept the different compliant level assistance according to the required bilateral motor patterns.
3) Based on the proposed biomimetic variable stiffness modulation strategy, a bilateral impedance control framework based on the inverse dynamics of the human–robot coupled system was implemented to realize the reference trajectory tracking. By transferring the biomechanics of the healthy side limb, the compliant patient–robot interaction can be achieved with the corresponding variable impedance characteristic, which was proved as the comparison results that with the increasing trends of the stiffness and damping values from 0 kg to 2.5 kg (average stiffness are 27.759 Nm/rad in 0 kg, 30.459 Nm/rad in 1.5 kg to 32.981 Nm/rad in 2.5 kg, and average damping are 3.68 Nm • s/rad, 3.85 Nm • s/rad, and 3.95Nm • s/rad), the average tracking errors show the decreasing trends (4.96 degrees, 4.06 degrees, and 2.77 degrees).

Therefore, the proposed biomimetic stiffness modulation strategy could regulate the output stiffness for enabling the

affected side limb perception of the bilateral motor skill pattern and relearning in different task intensities. Future works will focus on solving the influence caused by the uncertain terms of the system identification.

Data Availability All data collected and analyzed during this study are included in this paper.

Declarations

Conflict of Interest We declare that we have no financial and personal relationships with other people or organizations that can inappropriately influence the work reported in this paper.

References

1. Gerardin, E., Bontemps, D., Babuin, N. T., Herman, B., Denis, A., Bihin, B., Regnier, M., Leeuwerck, M., Deltombe, T., Riga, A., & Vandermeeren, Y. (2022). Bimanual motor skill learning with robotics in chronic stroke: Comparison between minimally impaired and moderately impaired patients, and healthy individuals. *Journal of Neuroengineering and Rehabilitation, 19*(1), 28. https://doi.org/10.1186/s12984-022-01009-3
2. Wu, J. Y., Cheng, H., Zhang, J. Q., Bai, Z. F., & Cai, S. F. (2021). The modulatory effects of bilateral arm training (BAT) on the brain in stroke patients: A systematic review. *Neurological sciences: Official Journal of the Italian Neurological Society and of the Italian Society of Clinical Neurophysiology, 42*(2), 501–511. https://doi.org/10.1007/s10072-020-04854-z
3. Chen, P. M., Kwong, P. W. H., Lai, C. K. Y., & Ng, S. S. M. (2019). Comparison of bilateral and unilateral upper limb training in people with stroke: A systematic review and meta-analysis. *PLoS ONE, 14*(5), e0216357. https://doi.org/10.1371/journal.pone.0216357
4. Sheng, B., Zhang, Y. X., Meng, W., Deng, C., & Xie, S. Q. (2016). Bilateral robots for upper-limb stroke rehabilitation: State of the art and future prospects. *Medical Engineering & physics, 38*(7), 587–606. https://doi.org/10.1016/j.medengphy.2016.04.004
5. Zhang, S. Y., Guo, S. X., Fu, Y. L., Boulardot, L., Huang, Q., Hirata, H., & Ishihara, H. (2017). Integrating compliant actuator and torque limiter mechanism for safe home-based upper-limb rehabilitation device design. *Journal of Medical and Biological Engineering, 37*(3), 357–364.
6. Curcio, E. M., & Carbone, G. (2021). Mechatronic design of a robot for upper limb rehabilitation at home. *Journal of Bionic Engineering, 18*(4), 857–871.
7. Chen, T. Y., Casas, R., & Lum, P. S. (2019). An elbow exoskeleton for upper limb rehabilitation with series elastic actuator and cable-driven differential. *IEEE Transactions on Robotics, 35*(6), 1464–1474.
8. Trigili, E., Crea, S., Moisè, M., Baldoni, A., Cempini, M., Ercolini, G., Marconi, D., Posteraro, F., Carrozza, M., & Vitiello, N. (2019). Design and experimental characterization of a shoulder-elbow exoskeleton with compliant joints for post-stroke rehabilitation. *IEEE/ASME Transactions on Mechatronics, 24*(4), 1485–1496.
9. Li, N., Yang, T., Yang, Y., Yu, P., Xue, X. J., Zhao, X. G., & Liu, L. Q. (2020). Bioinspired musculoskeletal model-based soft wrist exoskeleton for stroke rehabilitation. *Journal of Bionic Engineering, 17*(6), 1163–1174.
10. Wang, Y. W., Li, W. Y., Togo, S., Yokoi, H., & Jiang, Y.L. (2021). Survey on main drive methods used in humanoid robotic upper limbs. *Cyborg and Bionic Systems*, *2021*, 9817487.
11. Yang, Z. Y., Guo, S. X., Liu, Y., Hirata, H., & Tamiya, T. (2021). An intention-based online bilateral training system for upper limb motor rehabilitation. *Microsystem Technologies, 27*(1), 211–222.
12. Kim, R. K., & Kang, N. (2020). Bimanual coordination functions between paretic and nonparetic arms: A systematic review and meta-analysis. *Journal of Stroke and Cerebrovascular Diseases, 29*(2), 104544.
13. Kim, H., Miller, L. M., Fedulow, I., Simkins, M., Abrams, G. M., Byl, N., & Rosen, J. (2012). Kinematic data analysis for post-stroke patients following bilateral versus unilateral rehabilitation with an upper limb wearable robotic system. *IEEE Transactions on Neural Systems and Rehabilitation Engineering, 21*(2), 153–164.
14. Ballardini, G., Ponassi, V., Galofaro, E., Carlini, G., Marini, F., Pellegrino, L., Morasso, P., & Casadio, M. (2019). Interaction between position sense and force control in bimanual tasks. *Journal of Neuroengineering and Rehabilitation, 16*(1), 1–13.
15. Patel, P., & Lodha, N. (2019). Dynamic bimanual force control in chronic stroke: Contribution of non-paretic and paretic hands. *Experimental Brain Research, 237*(8), 2123–2133.
16. Jin, Y., Kim, M., Oh, S., & Yoon, B. (2019). Motor control strategies during bimanual isometric force control among healthy individuals. *Adaptive Behavior, 27*(2), 127–136.
17. Kim, H. J., Kang, N., & Cauraugh, J. H. (2020). Transient changes in paretic and non-paretic isometric force control during bimanual submaximal and maximal contractions. *Journal of NeuroEngineering and Rehabilitation, 17*(1), 1–11.
18. Kim, H. J., Lee, J. H., Kang, N., & Cauraugh, J. H. (2021). Visual feedback improves bimanual force control performances at planning and execution levels. *Scientific Reports, 11*(1), 1–10.
19. Yang, Z. Y., Guo, S. X., Hirata, H., & Kawanishi, M. (2021). A mirror bilateral neuro-rehabilitation robot system with the sEMG-based real-time patient active participant assessment. *Life, 11*(12), 1290.
20. Lodha, N., Coombes, S. A., & Cauraugh, J. H. (2012). Bimanual isometric force control: Asymmetry and coordination evidence post stroke. *Clinical Neurophysiology, 123*(4), 787–795.
21. Sun, C. Y., Chu, K. Y., Miao, Q., Li, P., Zhong, W. J., Qi, S. C., & Zhang, M. M. (2021). Bilateral asymmetry of hand force production in dynamic physically-coupled tasks. *IEEE Journal of Biomedical and Health Informatics, 26*(4), 1826–1834.
22. Leonardis, D., Barsotti, M., Loconsole, C., Solazzi, M., Troncossi, M., Mazzotti, C., & Frisoli, A. (2015). An EMG-controlled robotic hand exoskeleton for bilateral rehabilitation. *IEEE Transactions on Haptics, 8*(2), 140–151.
23. Teramae, T., Noda, T., & Morimoto, J. (2017). EMG-based model predictive control for physical human–robot interaction: Application for assist-as-needed control. *IEEE Robotics and Automation Letters, 3*(1), 210–217.
24. Pehlivan, A. U., Losey, D. P., & Oalley, M. K. (2015). Minimal assist-as-needed controller for upper limb robotic rehabilitation. *IEEE Transactions on Robotics, 32*(1), 113–124.
25. Asl, H. J., Yamashita, M., Narikiyo, T., & Kawanishi, M. (2020). Field-based assist-as-needed control schemes for rehabilitation robots. *IEEE/ASME Transactions on Mechatronics, 25*(4), 2100–2111.
26. De Luca, C. J., & Mambrito, B. (1987). Voluntary control of motor units in human antagonist muscles: Coactivation and reciprocal activation. *Journal of Neurophysiology, 58*(3), 525–542.
27. Fernandez, M. F. (2022). *A virtual muscle model of the arm for EMG-driven control of prostheses.* Doctoral dissertation of

Massachusetts institute of technology. Retrieved May 2022, from https://dspace.mit.edu/handle/1721.1/144594
28. Park, K., Kim, Y., & Obinata, G. (2012). Planning of bimanual movement training based on the bilateral transfer of force and proprioception by using virtual impairment. *Journal of Bioengineering and Biomedical Science, 2*(112), 2.
29. Cheung, V. C., d'Avella, A., & Bizzi, E. (2009). Adjustments of motor pattern for load compensation via modulated activations of muscle synergies during natural behaviors. *Journal of Neurophysiology, 101*(3), 1235–1257.
30. Roh, J., Rymer, W. Z., Perreault, E. J., Yoo, S. B., & Beer, R. F. (2013). Alterations in upper limb muscle synergy structure in chronic stroke survivors. *Journal of Neurophysiology, 109*(3), 768–781.
31. Stanev, D., & Moustakas, K. (2019). Stiffness modulation of redundant musculoskeletal systems. *Journal of Biomechanics, 85*, 101–107.
32. Wei, Q., Li, Z. J., Zhao, K. K., Kang, Y., & Su, C. Y. (2019). Synergy-based control of assistive lower-limb exoskeletons by skill transfer. *IEEE/ASME Transactions on Mechatronics, 25*(2), 705–715.
33. Furui, A., Eto, S., Nakagaki, K., Shimada, K., Nakamura, G., Masuda, A., & Tsuji, T. (2019). A myoelectric prosthetic hand with muscle synergy–based motion determination and impedance model–based biomimetic control. *Science Robotics, 4*(31), 6339.
34. Liu, Y., Guo, S. X., Yang, Z. Y., Hirata, H., & Tamiya, T. (2020). A home-based bilateral rehabilitation system with sEMG-based real-time variable stiffness. *IEEE Journal of Biomedical and Health Informatics, 25*(5), 1529–1541.
35. Li, H., Guo, S., Wang, H., & Bu, D. (2022), Subject-independent continuous estimation of sEMG-based joint angles using both multisource domain adaptation and BP neural network. *IEEE Transactions on Instrumentation and Measurement*, *72*, 4000910. https://doi.org/10.1109/TIM.2022.3225015
36. Yang, Z. Y., Guo, S. X., Liu, Y., Kawanishi, M., & Hirata, H. (2022). A task performance-based sEMG-driven variable stiffness control strategy for upper limb bilateral rehabilitation system. *IEEE/ASME Transactions on Mechatronics*. https://doi.org/10.1109/TMECH.2022.3208610
37. Liu, Y., Guo, S. X., Hirata, H., Ishihara, H., & Tamiya, T. (2018). Development of a powered variable-stiffness exoskeleton device for elbow rehabilitation. *Biomedical microdevices, 20*(3), 1–13.
38. Yang, Z. Y., Guo, S. X., & Liu, Y. (2021). Preliminary evaluation of a performance-based stiffness control for upper limb elbow joints rehabilitation. *In 2021 IEEE International Conference on Mechatronics and Automation (ICMA)* 1280–1285. IEEE.
39. Yang, Z. Y., & Guo, S. X. (2022). A hybrid motion stiffness control of variable stiffness actuator for upper limb elbow joints rehabilitation. *In 2022 IEEE International Conference on Mechatronics and Automation (ICMA)* 1324–1328. IEEE.
40. Ajoudani, A., Godfrey, S. B., Bianchi, M., Catalano, M. G., Grioli, G., Tsagarakis, N., & Bicchi, A. (2014). Exploring teleimpedance and tactile feedback for intuitive control of the pisa/iit softhand. *IEEE Transactions on Haptics, 7*(2), 203–215.
41. Dinh, B. K., Xiloyannis, M., Antuvan, C. W., Cappello, L., & Masia, L. (2017). Hierarchical cascade controller for assistance modulation in a soft wearable arm exoskeleton. *IEEE Robotics and Automation Letters, 2*(3), 1786–1793.
42. Lenzi, T., De Rossi, S. M. M., Vitiello, N., & Carrozza, M. C. (2012). Intention-based EMG control for powered exoskeletons. *IEEE Transactions on Biomedical Engineering, 59*(8), 2180–2190.
43. Day, J. M., Lucado, A. M., & Uhl, T. L. (2019). A comprehensive rehabilitation program for treating lateral elbow tendinopathy. *International Journal of Sports Physical Therapy, 14*(5), 818.